Systematic Study of Micro-Discharge Characteristics of ATLAS Barrel Silicon Microstrip Modules

T. Kuwano [a], K. Hara [a], S. Shinma [a], Y. Ikegami [b], T. Kohriki [b], S. Terada [b], Y. Unno [b]

[a] *Institute of Pure and Applied Sciences, University of Tsukuba, 1-1-1 Ten'nodai, Tsukuba, Ibaraki 305-8571, Japan*

[b] *High Energy Accelerator Research Organization (KEK), Oho 1-1, Tsukuba, Ibaraki 305-0801, Japan*

Abstract

One of the critical issues in fabricating silicon microstrip detectors is to suppress the micro-discharge, a rapid leak current increase when the bias voltage is raised. Among the 981 silicon microstrip modules fabricated by the ATLAS SCT Japan group, 111 modules showed the micro-discharge below 500 V bias at least once in the series of the quality assurance testing. We have conducted a systematic study to understand the causes, including the hot spot localization using an infrared sensitive camera, and measurement of leak current decay time.

Key words: silicon microstrip, ATLAS, SCT, micro-discharge, hot electron
PACS: 29.40.Gx, 29.40.Wk

1 Introduction

The ATLAS Detector is under construction for the LHC Collider Experiment to reveal the origin of the mass and to explore new physics in the regime provided by proton-proton collisions at 14 TeV center-of-mass energy. The Semiconductor Tracker (SCT) [1] [2] based on a technology of silicon microstrip is one of the three ATLAS Inner Tracking systems, PIXEL Tracker, SCT and Transition Radiation Tracker, located inside a 2-T magnetic field. The SCT

[1] Corresponding author. e-mail: hara@hep.px.tsukuba.ac.jp

consists of four concentric barrels in the central region, $30 < r < 60$ cm and $|z| < 80$ cm, and nine discs each in the forward/backward regions, $80 < |z| < 270$ cm, where r is the radial distance and z is the distance along the beam pipe from the collision point. The barrels are constructed from 2112 silicon microstrip modules that are identical in design. Each barrel module has four single-sided microstrip sensors, glued back-to-back on to a baseboard. The dimensions of the silicon sensors are 63.56×63.96 mm with a thickness of 290 μm. The strips of the two sensors on the same side of a module are wirebonded together, with a stereo angle of 40 mrad subtended between the top and bottom strips.

Twelve ABCD3T [3] binary readout ASICs are mounted on a hybrid based on a flexible Cu-polyimide circuit[4]. The hybrid reinforced with carbon-carbon backing bridges across the strips without touching the sensor surface nearly at the middle of the module, where the wirebonds to the strips and the bias lines are provided.

All the silicon sensors for the barrel modules were fabricated by Hamamatsu Photonics (HPK) using 4" process technology. There are 768 readout strips per sensor at a pitch of 80 μm. The p^+ implant electrodes 16 μm wide are biased through poly-silicon resistors of 1.5 MΩ. The readout Al electrodes 22 μm wide are AC coupled via SiO_2 and Si_3N_4 layers. The overhang design of Al electrodes over the implants moves the high edge electric field from the silicon into the oxide layer, hence reducing the risk of electrical breakdown.

The barrel modules were constructed at four qualified construction sites where a thorough quality assurance was carried out based on an agreed program. The program included metrology measurements, thermal cycling tests, electrical tests at -15 and 15°C where the test pulse system incorporated in the ABCD3T chips characterized the defective channels, and IV scans.

The IV, leak current vs. bias voltage, characterization is one of the critical test procedures. Among the 981 barrel modules constructed at the Japanese site, 111 modules showed a rapid leak current increase at a bias voltage below 500 V. Such a rapid current increase can be explained by a micro-discharge [5]. The drifting carriers are accelerated by the local high electric field, and generate multiple secondary electron-hole pairs, resulting in a rapid leak current increase. The local high field is often created in the vicinity of the strips where the field is maximum and any defects, if exist, increase the field further. Infrared radiation associated in the multiplication process could be viewed with an infrared sensitive (IR) camera as a hot spot, which can help localize the micro-discharge.

We have carried out a series of systematic measurements to characterize the properties of the 111 modules which recorded a degraded IV curve at least

once in the quality assurance procedure. For such modules, the SCT group has specified to derive the leak current decay time when the module is kept at 500 V bias. Adding to this test, The Japanese Group tried to localize the hot spot with an IR camera and to identify any visible traces associated. The noise distribution available from the electrical tests was also utilized to compare with the visual and IR information. The sensor leak current specification to the manufacturer was defined in the bias range below 350 V, while we extended the maximum up to 500 V. Therefore some sensors accepted at delivery showed the micro-discharge in the extended bias region. Because of this and of the fact that HPK can produce sensors with much superior IV characteristics with 6" process [6], the present study may provide limited information only specific to our case, the fraction of micro-discharge sensors, for example. However, the systematic study presented here covers the general micro-discharge properties. The results should be useful to understand its origin, and hence to suppress the micro-discharge occurrence in future sensor manufacturing.

2 IV and hot spot measurement procedures

2.1 IV measurements

The requirement to the leak current per sensor is less than 2 μA at 350 V when the current is scaled at 20°C. The IV per sensor was scanned at about 25° room temperature and 50% humidity by HPK. Most generally the leak current was less than 0.2 μA with a distribution peak around 0.13 μA at 350 V. The sensors were IV tested up to 500 V before they were assembled into modules. The sensors which showed substantially larger currents were grouped and used in a same module so that the number of micro-discharge modules is kept small.

The module IV scan is a part of the common electrical test procedure. The measurement took place at least four times before the module shipment. The first module IV scan was taken at 15°C and 59% humidity at the module construction sites, HPK and SPI (Seiko Precision Inc.). The other IV tests were performed at KEK once at -16°C and twice at 15°C. At KEK, up to 12 modules were tested together in a light-tight thermostat chamber flushed with dry N_2. The bias voltages were supplied through SCTHV [7] modules housed in a VME crate. The SCTHV modules and other VME modules were configured as an SCTDAQ system [8], common among the construction sites. SCTHV module can monitor the currents with a precision of 1% readings or 20 nA. The leak current was measured up to 500 V with a step of 10 V or 15 V. The current was read out 10 s after the bias was stepped up.

Additional IV scans were performed for the modules with abnormal IV using the SCTDAQ system or a small PC-PCI/GPIB based system. In the PC-PCI/GPIB system, a single source meter (Keithley 6517) was used for biasing up to six modules. The individual module current was evaluated from the voltage drop across a 1 MΩ resistor. A scanner card implemented digital multimeter (Keithley 2010) was used to scan over the six modules. The same system was used to measure the 24 h leak current to extract the leak current decay time.

The thermostat chamber in the tests was usually flushed with dry N_2, which is the same condition as in the real ATLAS experiment. In order to examine the dependence of the micro-discharge onset voltage on humidity, the IV curves of 15 micro-discharge modules were compared at 0% and 50% humidities. The micro-discharge onset voltage, typically at 450 V at 0% humidity, shifted upwards and disappeared for 12 modules at 50% humidity. The suppression of the micro-discharge in humid condition can be explained by that the sensor surface should become more conductive at higher humidity, which acts to relax the charge multiplication associated in the micro-discharge process.

We then studied the temperature dependence, comparing the IV curves of six micro-discharge modules at temperatures 15 and 25°C with all at 0% humidity. The leak current of Si sensors should increase to 2.4 times in this temperature increase. The micro-discharge leak current, however, turned out not to increase but decrease by typically 10% from 15 to 25°C. The onset voltages were found not to change in these temperatures. The charge multiplication should become large at lower temperatures, since the acceleration is achieved further due to less thermal disturbance. The present observation is qualitatively consistent with this expectation.

2.2 IR hot spot measurements

The IR measurement system is based on the Hamamatsu back-thinned 512×512 pixel CCD chip with C4880 controller. The device provided 16-bit imaging with a quantum efficiency of 92% at 650 nm and 10% at 1000 nm. The CCD was cooled to −55°C by the Peltier to reduce the dark current noise. The device was attached to a vertical stage in order to provide focusing at the test module which was placed about 40 cm apart. The whole setup was placed in a light-tight box.

The rms noise evaluated from fluctuations in the background pictures was 3 electrons/pixel/sec, and was negligible. It turned out, though, that a certain noise pattern existed. The influence of this extra background was minimized by subtracting the images with and without bias, both being exposed for the

same period. The exposure time was up to several minutes, depending on the intensity of the hot spot and the lens magnification.

The hot spot search started with the wide-angle lens which covered the area one half of the module. The micro-discharge module was therefore exposed four times to survey the hot spots. The hybrid, 2.1 cm wide bridging over the module, hides the sensor surface and the corresponding area, 16% of whole area, could not be surveyed: all the bonding pads were under full exposure. Once a hot spot was detected, the detailed position was determined using a microscope lens. The most expanded image covered a region of about 600 μm square. Any visible traces were then examined with a conventional microscope. Some visible characteristic pattern was required in the IR images for this procedure.

The module bias was adjusted such that the leak current was in a range of a few μA. The ADC of CCD imaging, 16 bits, overflowed if the exposure time was set too long. With the wide-angle lens, the optimum exposure time was 1 min for $\sim$3 μA leakage and 5 min for $\sim$1 μA leakage. With a microscope lens, the exposure time was around 30 s.

3 Results

3.1 Micro-discharge onset voltage

The IV curves of the first 200 modules are shown in Fig. 1. Most of the modules showed the pattern (A) where the leak current increased rapidly up to the full depletion voltage ranged between 50 to 90 V, and then increased slowly up to 500 V we measured. The micro-discharge onset voltage of pattern (B) was defined as the lowest voltage which deviated from the smooth curve of pattern (A). The voltage was unambiguously determined except for 6 modules where the current increased monotonically starting below the full depletion voltage, pattern (C). A few 10 V of the onset voltage was assigned for these modules. The total number of micro-discharge modules we identified is 111. Figure 2 histograms the onset voltages of the 111 modules. Among these, 80 (72%) modules have the onset voltage above 400 V, 23 (21%) modules between 200 and 400 V, and 8 (8%) modules below 200 V.

Out of the 111 micro-discharge modules, we succeeded in identifying hot spots for 61 (55%) modules. Some modules showed multiple number of hot spots in different sensors or apparently different types of hot spot traces. They were counted separately: the number of hot spots counted 72 in total.

Table 1 lists the numbers of 72 hot spots (61 modules) classified based on the types of traces and the locations. The two modules in Type O) are recorded to be damaged and the traces are obvious. The rests of the 70 identified hot spots are located mostly near the strip edges: only two were found around the bias-ring edge and three around the wirebonding pad edge. In all cases, the hot spots are located at the structure edges where the electric field is largest.

Photographs of typical hot spot types are shown in Fig. 3. In type A), the hot spot is located at the sharp edge of irregularly shaped p^+ implant. Such irregularity was caused by improper lithography for the ion bombardment. Types B) has scratch-like irregularities running underneath the Al strip. Such scratches have been created while oxide or nitride layers were created. Type C) shows a cluster of dots along the Al strip edge. The Al strip edges are clear, meaning that Al deposition was done properly but rinsing was not sufficient. Although the visible anomaly is not spectacular for type D), some colored dots are seen in the oxide/nitride layers, a few μm away from the Al strip edge. The dots are created by droplets of photoresist resin. Eight modules (12%), type E), show no trace of irregularity at the hot spot.

The above classification is based on the images of the conventional microscope, because the IR images are not distinct enough to perform detailed classification. In taking conventional images, we relied on nearby characteristic pattern so as to localize the hot spot position. In type G), no characteristic pattern was found in the IR image. In type F), we found some traces in the IR image but did not allow further classification based on conventional images for scheduled shipping.

Excluding the two Type O) modules, the rest have sensor-process originated problems, 41 Types A) to D) modules with clear traces of flaw, and 20 Types E) to G) modules without.

Four among the 50 hot spot unidentified modules have recorded damages during module fabrication and testing. The damaged modules count six in total adding the two Type O). The leak current for 19 modules did not exceed 1 μA, and the hot spot is too tiny to detect. In fact the onset voltages for these distribute mostly around 500 V (see Fig. 2).

The remaining 26 modules had a large enough leakage exceeding 1 μA. We

categorize these as "Dark" modules. Taking into account of the area hidden by the hybrid, some 10 modules could be considered to have hot spots located behind. This implies that some 16 modules need to be accounted for the cause of micro-discharge and why the hot spot is not visible. The distribution of micro-discharge onset voltages for the "Dark" modules is not much different from the rest, as shown in Fig. 2. Among the 6 modules with very small onset voltage, hot spots were found successfully for 3 modules (Modules 706, 917 and 958). Module 706 has corrosion-like dots of $\sim$60 μm length along the Al edge, Type C), see Fig. **??**. Modules 917 and 958 are damaged during module production, Type O): 917 has a dimple of $\sim$150 μm width. The three other modules are damaged during module fabrication or testing, and the damaged are obvious.

3.3 Electrical noise

The measurement of the amplifier input noise (ENC) is a part of the agreed common test procedure but at a bias of 200 V. The noise levels of micro-discharge modules were measured in addition setting the bias above the onset voltage. The noise level is typically 1500 e^- for genuine channels. The micro-discharge module shows usually a cluster of about 5 to 7 noisy channels about the hot spot channel. Among the 61 hot spot identified modules, or 72 spots (100%), 56 spots (78%) showed consistent noise distributions centered at the hot spot channels. The remaining 16 spots are not associated with noisy channels.

The noise distributions for the "Dark" modules are found also to be consistent with micro-discharge. Among 13 "Dark" modules with onset below 375 V, only one module showed no noisy channel.

3.4 Micro-discharge history in the test sequence

The micro-discharge could potentially be created in many handling processes involved in the module production and testing. Actually, we almost eliminated the procedure where the sensor strip side was touched directly. The sensors were slid on to the alignment tables [9] with the strip side up, avoiding use of vacuum tweezers. When the aligned sensors were transferred to the gluing jig, the strip side was vacuum chucked but through a porous clean-room paper. No glue was applied on the sensor strip side. Finally, the only jig that touched the strip face was the wire bonding head.

The fabricated module was kept in an aluminum box for protection. For metrology measurement, the modules needed to be taken out to another frame.

Unfortunately a couple of modules were damaged by accident creating obvious scratches on the surface.

Figure 5 shows the evolution of the number of micro-discharge modules counted at the tests in sequence. The test sequence [2] consists of five steps, "sensor", "module", "LT", "LTL" and "final". Brief descriptions of the tests, and the temperature and humidity conditions are described in the figure caption. Among the 111 micro-discharge modules, 71 modules were fully tested in the specified sequence: the rest were not IV tested on individual sensor up to 500 V, or the tests were swapped in sequence. The evolutions are shown separately for all of these modules, 32 modules (among the 71 modules) whose hot spots were not identified, and 24 modules (among the 32 modules) with leakage larger than 1 muA ("Dark" modules). In the chart, the modules are grouped either micro-discharge is already seen in the previous test or new, and the same fill patterns show the evolution of these numbers. For example in the chart a), 14 modules are new at "LT", while 31 are since "module" and 21 are since "sensor".

The first test "sensor" is not on the modules but on individual sensors. There are 74 modules that are assembled using at least one micro-discharge sensor. Among this, 22 modules showed micro-discharge in the later tests, and 52 did not show any since assembled. These 52 modules are not categorized to micro-discharge, which are shown in broken lines. The reduction from 74 to 22 can be explained qualitatively that boding the Al electrodes to the ASIC inputs stabilizes the electric field to suppress the micro-discharge development owing to the extended electrode design.

The number of once identified micro-discharge modules is not identical, because the modules with onset voltage close to 500 V have some probability to fluctuate when the test is repeated. In this view, the numbers at "LT" and "final" can be regarded unchanged. The number dropped slightly at "LTL". This tendency is consistent with that the micro-discharge is suppressed at lower temperatures. At "LT", 14 modules were new and the number 7 at "module" increased to 21, which can be qualitatively understood by the humidity change from 50% to 0%.

Among the 32 modules new at "module", 20 modules showed IR hot spots and the sensor process originated problems are evident. Since the humidity conditions at "sensor" and "module" are similar, we conclude that the sensor micro-discharge developed in this period.

3.5 Micro-discharge decay time

The local high electric field responsible to the micro-discharge has a tendency to be tendered with time. The SCT group has specified to evaluate the leak current decay time by keeping 500 V bias for 24 h. The leak current decay appeared to follow an exponential function approaching to an asymptotic value for most of the modules. The decay time constant is defined as the time constant of the exponential. The time constant could not be derived for 3 damaged modules because the leakage decayed initially but increased later, or it was not stable.

The time constants are plotted against the initial leak current in Fig. 6. The hot-spot identified modules are marked with crosses in the figure. We notice a general tendency that the decay time is longer if the initial leakage is larger. There are exceptions, though, that have a longer decay time ($>\sim$1 h) irrespective of the initial leakage, and the probability of finding "Dark" modules is larger in this group. This observation is reasonable since instantaneous intensity is smaller for the long lived hot spots.

Although the reason for the "Dark" modules is not fully understood, they are probably usual micro-discharge modules but the leakage decay time is longer: Not anomaly is found in their noise distributions and history in the test sequence. The reason for the longer decay is investigated from the photographs of the IR luminous modules with longer decay. They tend to have no flaw associated or mild flaws with no sharp edges.

3.6 Installation to the SCT Barrels

The observation that the micro-discharge decays with time led us to install those modules with the onset voltage and the decay constant within predefined values. The SCT group decided to place micro-discharge modules on the outer barrels where the radiation environment is less severe and the operation voltage will be kept moderate. Following the criteria specified by the SCT group [2], 97 micro-discharge modules have been shipped for assembling into the barrels: 83 modules (with micro-discharge onset voltage $V_{MD} > 350$ V and the leakage decay time $T_{MD} < 1$ h) are for the outer 3rd or 4th barrels. 14 modules with $150 < V_{MD} < 350$ V and $T_{MD} < 6$ h are kept as spares. The remaining 14 modules are regarded as fail and will not be used.

4 Summary

ATLAS Japan SCT Group has completed production of 981 barrel modules, among which 111 modules were found to show a rapid increase of leak current at a bias below 500 V at least once in the series of the quality assurance tests. Among 111 modules, six have been damaged at module handling. Investigation through IR hot spot imaging was successful for 59 other modules. About 2/3 of them have problems evident in the sensor, related to photoresist processing and cleaning. The rest must also have sensor originated problems but are not associated with clear visible flaw.

Concerning 47 modules which were failed to identify IR hot spot, 2/5 were tiny micro-discharge modules with the onset close to 500 V. The rest have a noise distribution consistent with of IR luminous modules but tend to have longer leakage decay constant.

Since the micro-discharge is influenced by the humidity, the sensor IV measured at 50% humidity is not always consistent with the module IV measured in dry N_2. Also the sensor seems to develop micro-discharge with time in the earlier stage of the test.

References

[1] K. Kondo et al., Nucl. Instrum. and Methods A 485 (2002) 47; ATLAS Inner Detector Technical Design Report, CERN/LHCC 97-16, CERN/LHCC 97-17, 1997.

[2] ATLAS SCT barrel group, The Barrel Modules of the ATLAS SemiConductor Tracker, paper accepted for publication in Nucl. Instrum. and Methods A.

[3] W. Dabrowski, et al., Proc. of the Sixth Workshop on Electronics for LHC Experiments, CERN/LHCC/2000-41, p.115.

[4] Y. Unno, et al., Nucl. Instrum. and Methods A 541 (2005) 286; Y. Unno, Proc. of Sixth Workshop on Electronics for LHC Experiments, CERN/LHCC/2000-41, p.66.

[5] T. Ohsugi, et al., Nucl. Instrum. and Methods A 342 (1994) 22.

[6] T. Akimoto, et al., IEEE Trans. Nucl. Sci. 51 (2004) 1546.

[7] Gornicki, S. Koperny, P. Malecki, SCTHV VME Model 203 User's Manual, Institute of Nuclear Physics PAN, Cracow, Report 1947/E, July 2004.

[8] D. Robinson, Nucl. Instrum. and Methods A 485 (2003) 84: A. Ciocio, Nucl. Instrum. and Methods A 541 (2005) 259.

[9] Y. Kato, et al., Nucl. Instrum. and Methods A 511 (2003) 132.

Table 1
Classification of hot spot images. Since multiple hot spots are identified in a module, numbers in terms of hot spots are given in parentheses in addition to the numbers in terms of modules. (The sum of modules is 63, since two modules are classified into two different categories)

Number of micro-discharge modules	111	
Number of modules with hot spot identified	61	
Number of hot spots		(72)
O) obvious damage by mis-handling	2	(2)
A) implant is irregularly shaped	7	(13)
B) scratch-like trace underneath Al	7	(7)
C) cluster of dots along Al edge	5	(6)
D) dots in oxide/nitride layer	22	(24)
E) no visible trace is identified	8	(8)
F) some trace (not classified)	3	(3)
G) no obvious trace (not classified)	9	(9)
hot spots at the strip edges	58	(67)
hot spots at the bias-ring	2	(2)
hot spots at the bonding pad edges	3	(3)

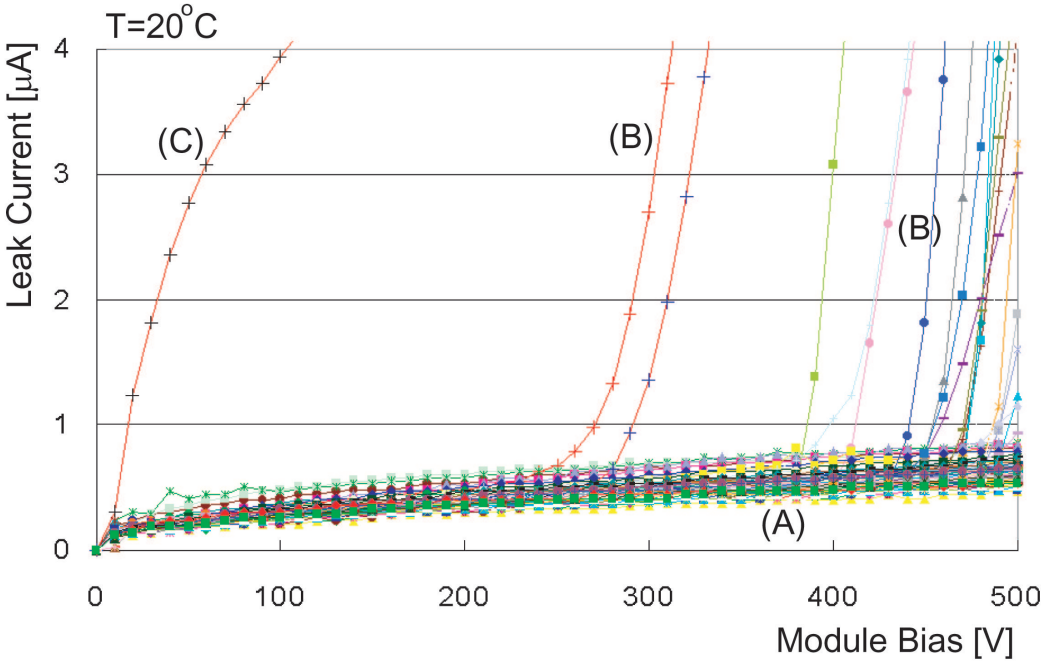

Fig. 1. *IV* curves of Module 1 to 200. The leak current is normalized to 20°C.

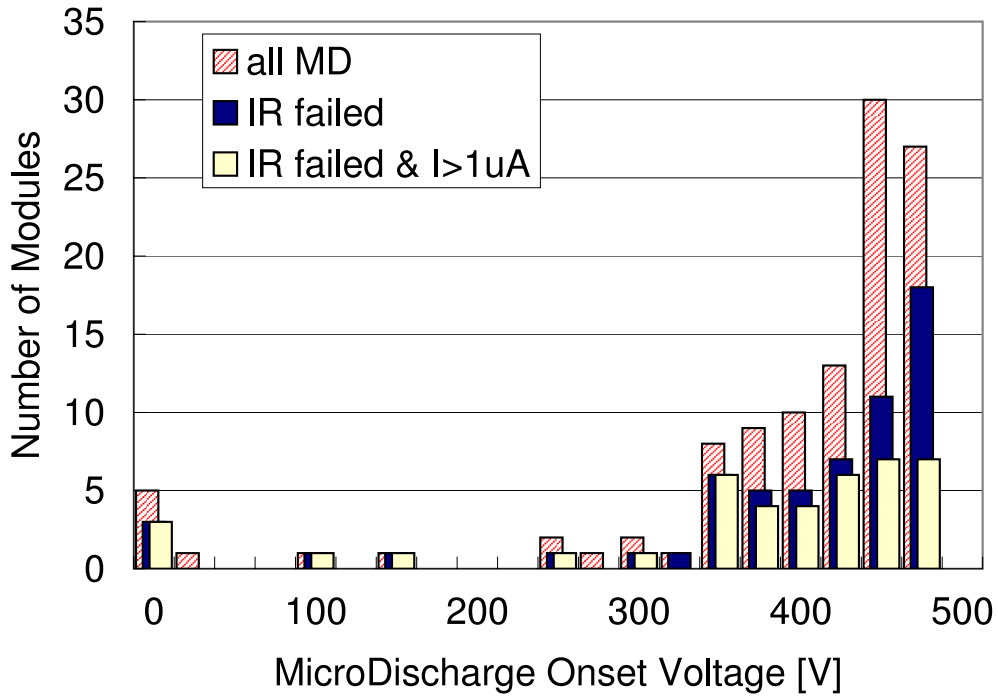

Fig. 2. The micro-discharge onset voltages for all 111 modules. The subset for 61 modules whose hot spots are identified by IR camera are shown in dark histogram. Among 61, the leakage is greater than 1 μA for 30 modules, shown in open histogram.

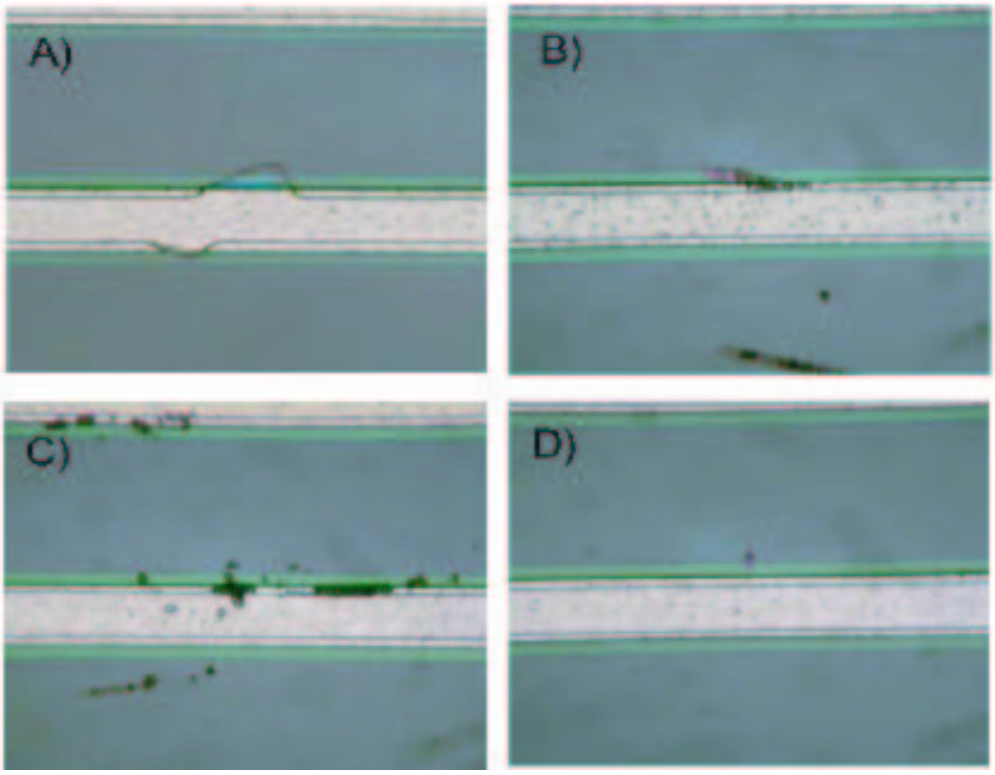

Fig. 3. Four typical types of hot spot sources. The sources are located at the center of each photo. The horizontal white strip is the Al electrode. The parallel two lines inside Al show the boundary of the p^+ implant underneath. A) The implant is irregularly shaped; B) Scratch-like traces traversing underneath the Al strips (another trace is visible at the bottom); C) Clusters of dots are located along the Al edge; D) A dot (or clusters of dots) is visible in oxide/nitride layer apart from the Al.

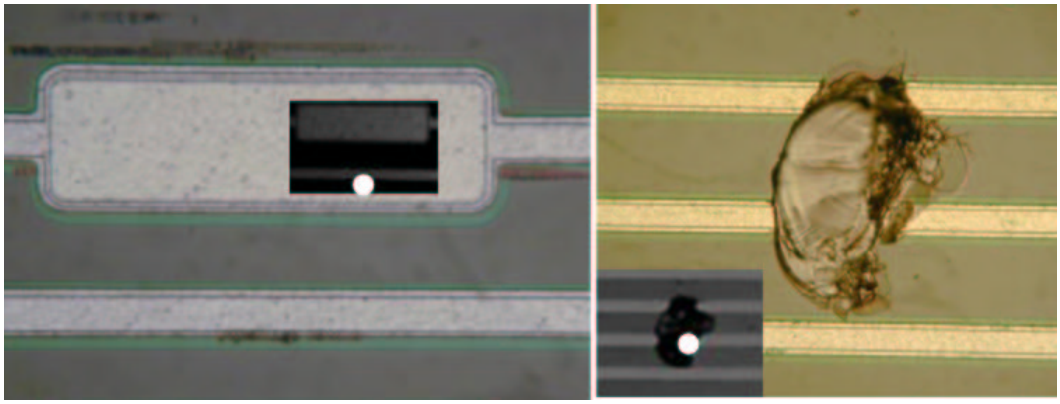

Fig. 4. Two modules with micro-discharge onset voltage of almost 0 V. The white spot in the IR image shows the hot spot location. (left) sensor process problem and (right) damaged.

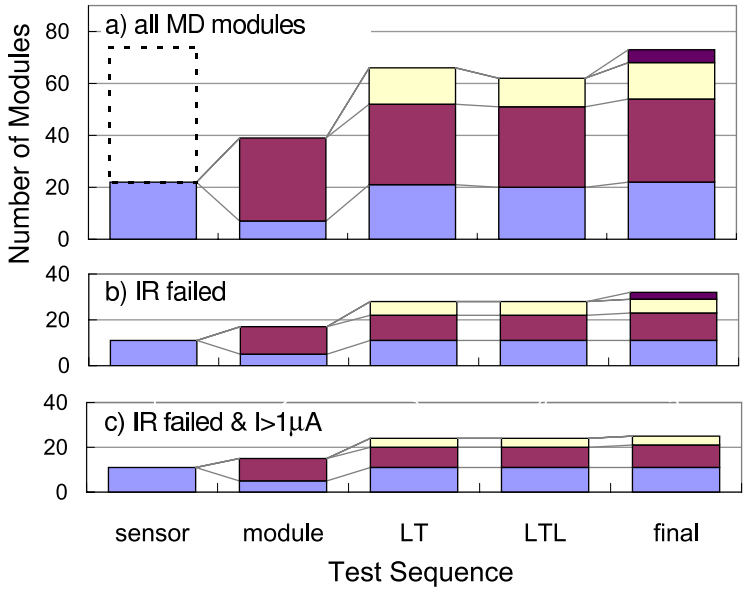

Fig. 5. The numbers of micro-discharge modules counted at each test in sequence. The test "sensor" is for individual sensor IV made prior to assembling into modules (25°C and 50% humidity), "module" is the test at the module assembly sites (15°C and 50%), "LT" (15°C and 0%, 20 h long-term stability test), "LTL" (−16°C and 0%, low temperature test), and "final" (15°C and 0%, before shipping) are the tests done at KEK. a) 71 micro-discharge modules tested in the specified sequence. b) subset of a) with IR hot spot not identified. c) subset of b) with the leakage larger than 1 μA.

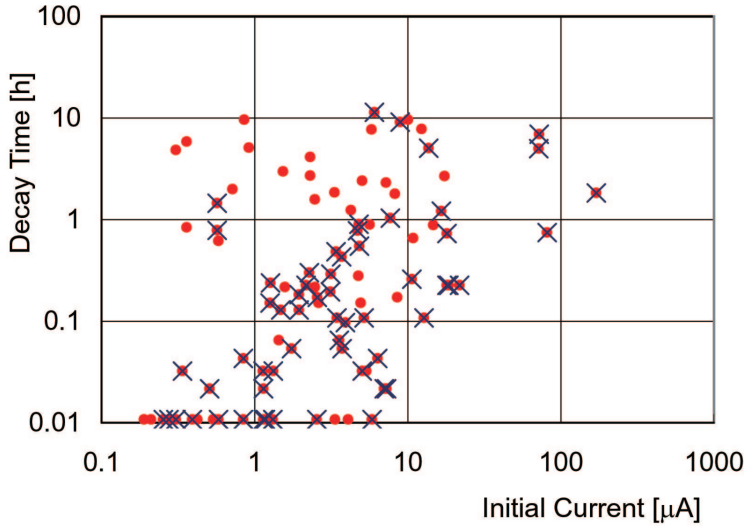

Fig. 6. The correlation between the current decay time constants and the initial leak current, measured for 108 modules. Crosses are attached to the 61 modules whose hot spots were identified.